N000142312053 : DRI The Arabian Sea Transition Layer (ASTraL) Exchange across the Air-Sea Interface

Reporting Period: OCT 01, 2023 to SEP 30, 2024

Date Received:

Submitter: Harindra Fernando

Distribution Statement: Approved for public release; distribution is unlimited.

Major Goals

Every year during March to May a compact region of elevated Sea Surface Temperature (SST > 30 degrees C) develops in the Southeastern Arabian Sea (SEAS). This phenomenon is believed to have strong implications on biophysical interactions and underwater acoustics in the Arabian Sea (AS) as well as initiation of boreal summer Southwest (SW) monsoons. Known as the Mini Warm Pool (MWP) because of its smaller size compared to other warm pools in the world, MWP develops over an area with solar insolation comparable to the rest of the AS, which suggests that a myriad of interacting multiscale atmospheric and oceanic processes is responsible for MWP. This project conducts research on dynamical process underpinning the lifecycle (genesis, maturation, and dissolution) of MWP by participating in the ONR-ASTraL (Arabian Sea Transition Layer) Departmental Research Initiative. The origins of MWP can be traced to the collapse of summer SW monsoons of the yesteryear, during which oceanic coastal planetary [Kelvin] waves are generated in the Bay of Bengal. These waves together with low saline water arriving in SEAS during the winter Northeast monsoons produce a large anticyclonic eddy in SEAS, signifying a downwelling Rossby wave. This feature, known as the Lakshadweep high (LH), is the hub of MWP.

Accompanying and evolving physical processes underlying MWP are numerous: the formation of a thicker and warmer barrier layer topped by a thin low-salinity colder surface layer separated by a pycnocline, air-sea interactions regulated by boundary layers above and below the ocean surface [together known as the transition layer], development of a low-level westerly jet and its instabilities, and development of deep convection in SEAS that finally leads to the Monsoon Onset Vortex.

Four guiding hypotheses are proposed to undergird the data analysis, and they concern: (i) the development of MWP during the evolution of air-sea fluxes in the transition layer due to evolving large-scale environmental forcing and micro-scale response thereof; (ii) warming of the thin upper mixed layer of LH via entrainment at the pycnocline, temperature inversions and lateral processes; (iii) generation of the SW monsoon onset vortex as a result of instabilities of the low-level westerly jet, and amplification of resulting cyclonic vortex via enhanced turbulence and fluxes ensuing from deep convection and breakdown of instabilities; and (iv) rapid dissolution of MWP with the SW monsoon onset due to a combination of intense upper ocean turbulence, development of mesoscale structures and propagating planetary waves (e.g., westward migration of LH).

These four hypotheses will be tested, and relevant research questions are to be addressed by participation in all three ASTraL field campaigns in 2023 (completed), 2024 (completed) and 2025 (pending), wherein an extensive suite of atmospheric and oceanic instruments will be deployed by University of Notre Dame (UND) group. Meso- and micro-scale processes active in MWP will be further investigated using a novel large eddy simulation (LES) approach by a Principal Investigator from the National Center for Atmospheric Research (NCAR), whose focus will be on the impact of ocean heterogeneity on transition layer. Collaboration with southeast Asian nations (India, Sri

Lanka, Maldives), Naval Research Laboratories (NRL, Monterey and Stennis) and other ASTraL PIs are sought, building upon existing partnerships. Training of STEM students, post-doctoral fellows, early career scientists and technical staff will be an integral part of the project. The results will be published in archival journals, and disseminated via presentations in national and international conferences.

During FY-2024, UND participated in the second ASTraL cruise, and gathered an extensive set of data. Given the geopolitical situation, unfortunately, the cruise was conducted in the Bay of Bengal (BoB), away from the SEAS-MWP. A tropical cyclone -- Remal – perceived to be related to monsoon onset was observed, and the data processing and interpretation were mainly replated to the observations following Remal. Therefore, the data gathered were mainly analyzed to study the behavior of the vortex.

NCARs collaborative computational research with UND focused on air-sea interactions studies using LES, in particular, the impact of ocean heterogeneity on atmospheric and oceanic boundary layer (ABL, OBL) dynamics. Ocean heterogeneity specifically refers to horizontal gradients in SST and currents, which arise naturally due to an abundance of mesoscale and submesoscale ocean fronts and eddies. Process studies and phenomenological discoveries were at the heart of the computational component. Simulation results are complimentary to observations, and they could be used as guidance for collecting and interpretation of field data. Over FY-2024, developing and exercising a new coupled atmosphere-ocean LES code was a major task. It leveraged developments started during MISO-BOB that utilized the Message Passing Interface to run multiple LES simultaneously. In its present configuration, the code runs atmospheric and oceanic LES with coupling routines that link the simulations in the following order at each time step: (i) Interpolate the currents and SST from the OBL to the first model level in the ABL; (ii) surface fluxes are then computed in the ABL; and (iii) then ABL surface fluxes are interpolated and communicated to the OBL.

Accomplishments Under Goals

Highlights of UND and NCAR Research:

(i) UND participated in both Leg 1 (27 April to 14 May) and Leg 2 (18 May to 16 June) of the 2024 cruises aboard Thomas G. Thompson (TGT). The instruments used are listed in Table 1 (uploaded document). Most data taken were high resolution/frequency. The mobilization occurred in Fremantle, Australia (Fig. 1). Instruments were operated continuously during Leg 1 and Leg 2, except in EEZs. Radiosondes were launched six-hourly in Leg 1 and four-hourly in Leg 2 (Fig. 2a, b). UND also operated the NOAA flux tower at the bow. The TGT track for the Leg 1 followed a north-south transect of the Bay of Bengal during the pre-monsoons. The Leg 2 was designed for capturing atmosphere-ocean transition layer processes in BoB.

(2) During Leg 1, the TGT track shows three distinct regimes (Fig. 3, top): (A) Dry subtropics (12N - 17N), (B) Transition zone (6N - 12N), and (C) ITCZ (2N - 6N). In (A), very dry free troposphere topped a very shallow (300-400 m) and moist boundary layer with a moist static energy (MSE) maximum (Fig. 3a-c). Soundings (Fig. 4a) show a dry temperature inversion at the ABL top, with a MSE minimum atop a surface MSE maxima due to dry air from the Indian landmass. Regime (B) was characterized by mixed-layer growth (~ 1km; Fig. 3a), colder easterly winds that dissolve inversion (Fig. 3b, 4b), dry mid and upper troposphere (Fig. 3a), increase of MSE in mid/upper troposphere (Fig. 3c) and passing showers (Fig. 5). In (C), the entire atmospheric column is moist (Fig. 3a, 4c) and favorable for moist convective activity (higher MSE in upper troposphere) and wind shear – westerly in the lower and easterly in the upper troposphere. The mixed layer (depth ~ 700-1000 m) lowered after the rainfall events (Fig. 3b).

(3) The CL61 ceilometer indicated that in subtropics (Case A) aerosols (from depolarization ratio) were trapped in a shallow layer (Fig. 6 a,b), capped by cumulus clouds (attenuated backscatter), especially during nocturnal periods. In the transition regime (Case B), the cloud tops reached ~ 3 km, consistent with the low MSE altitudes (Fig 6 c,d). In the ICTZ (Case C), the clouds were deeper with heavy and frequent precipitation. Ice-phase clouds occurred only in Case C (Fig. 6 e,f).

(4) During Leg 2, the winds could be categorized based on the development of tropical cyclone Remal in the northern BoB (Fig. 7): Pre-Monsoon (18-21 May; easterly wind speeds 1-5 m/s in the entire troposphere); Tropical Cyclone or Depression (May 22 – May 27; westerlies exceeding 8 m/s in the troposphere); Recovery (28 May 28-02 June; ~ 2-4 m/s in the lower troposphere, and < 1 m/s between 2-5 km); and Monsoons (03 -13 June). Our analysis for FY24 concerned the Tropical Cyclone Heat Potential (TCHP) and the Recovery phase. The former is the vertically integrated heat content per unit area above the isotherm 26 °C, which is the temperature below which hurricanes do not form. When SST is cooled below the air temperature, energy is not readily extracted from the sea and a hurricane can no longer be sustained. When TCHP > 60 kJ/cm2, tropical-cyclone (TC) intensity increases (Mainelli et al., Weather and Forecasting, 23(1), 3–16, 2008). NOAA recognizes that regions of TCHP> 90 kJ/cm2 are most likely to cause sudden TC intensification. The TCHP in Fig. 8 are broadly consistent with the above estimates.

(5) The cloud top brightness temperature (CTBT) was obtained from the INSAT-3D satellite. Lower CTBT (more negative) signify higher vertical development and greater intensity of convection. During the recovery period the skies remained clear, with minimal deep convection (Fig. 9). Precipitation events were evident from INSAT-3D throughout the entire cruise, except during the Recovery phase. This was confirmed by ODM 470 disdrometer (Fig. 10). (6) Fig. 11a illustrates the relative humidity profiles derived from radiosonde observations, overlaid by cloud base heights from CL61. A dry slot of air above the ~ 3km altitude is seen, indicative of a northeasterly intrusion (Fig. 11b) during the Recovery phase. Wind speeds within the dry slot were consistently below 2 m/s (Fig. 7). ERA5 reanalysis (not shown) indicates that this dry slot previously prevailed over the Indian subcontinent and the Arabian Sea, before being advected towards the BoB. A westerly wind regime with comparatively high speeds dominated around 25°N latitude, which transitioned into a northeasterly flow with the onset of summer monsoon (based on ERA5 reanalysis data).

(7) Before the Tropical-Cyclone phase, the marine ABL height remained ~ 0.6 km throughout the day (Fig. 12a). With the passage of cyclone, however, deep convective events occurred and the ABL grew as high as 3-3.5 km (Fig. 12b). During the Recovery phase, the diurnal cycle was evident, facilitated by low winds, and the ABL height varied between ~ 600 m at night and 1.5 km during the day. The most notable during the Recovery phase was the presence of layered structures extending up to ~2.5 km in altitude (Fig. 12c), which disappeared during the post-Recovery (Monsoon) phase (Fig 12d). Figs. 13 show an expanded view of backscatter with layering, over a day (Fig. 13a,b) and at a given hour (Fig. 13c,d), respectively. Fig. 13b shows the linear depolarization ratio, indicating the aerosol presence only up to the top of the boundary layer ~ 0.6 km. Together, Figs. 13a-d show that layered structure above ABL is due to density layering, perhaps due to shear-induced vertical mixing in the region of stronger stratification found at 1- 3 km. A mechanism of layer formation in marine ABL during turbulent overturning events has been proposed by Fernando et al. (Environmental Fluid Mechanics, 23(2), 489-510).

(8) The NCAR coupled ABL-OBL code was exercised over a range of unstable atmospheric stability ranging from free convection to nearly neutral for ``nominally” heterogeneous boundary layers. Nine coupled ABL-OBL simulations were completed with changes in ABL stability (by changing geostrophic winds) and setting the initial temperature jump between the ABL and the ocean SST. The ABL-OBL are coupled through the surface currents, momentum fluxes and an energy balance that includes sensible and laten heat fluxes. Results show coupling across a wide spectrum of scales

ranging from meters to kilometers. For example, Fig. 14 shows a large downdraft generated from a shear-convective roll (SCR) in the ABL impinging on the ocean surface, while at the same time Langmuir turbulence generates its own smaller scale downdraft-updraft pairs in the OBL. SCRs are long lived ABL structures with their axis roughly aligned with the mean wind. At the ocean surface their spanwise organization generates fluctuations in the surface momentum stress, leaving a persistent imprint on the ocean at large scales (Fig. 15).

(9) The impact of organized ABL structures on OBL was evaluated by comparing simulations that use instantaneous point-by-point spatial coupling rules versus similarly configured simulations that use spatially (x-y) average coupling rules. The LES show large-scale spatially intermittent turbulent structures in the ABL that modulate SST, currents and momentum and temperature fluxes. The power spectra in OBL, computed in the spanwise direction, show a large peak at the scale of the SCR. Fig. 16 shows that entrainment flux is approximately -0.2 of the surface heat flux at the ABL top, which is consistent with previous atmospheric convection work. Conversely, Langmuir turbulence increases the OBL entrainment by nearly a factor of three compared to its ABL counterpart. Thus, Langmuir turbulence may contribute to the sudden collapse of the Arabian Sea MWP under increasing winds.

(10) A five-year MOU was signed between the Ocean University of Sri Lanka, National Aquatic Resources Research and Development Agency (NARA, Sri Lanka) and UND, upon receiving Approval of the Sri Lanka Cabinet (https://efmlab.nd.edu/news).

Plans Next Period

The major activity for the next reporting period for UND is the participation in the EKAMSAT-2025 cruise. Theirs is a joint deployment with NRL (Monterey) and NRL (Stennis), and an array of complementing instruments are planned. Currently the logistics are being worked out, considering the geopolitical shifts in the Indian Ocean and Arabian Sea, for which UND play a key role. Training of STEM students is also a key task, in the field and in academic endeavors. Devmi Gamage and Selina Bolella will continue to conduct research on the ASTraL project as a part of their PhD thesis research. Several papers are in preparation, which UND hopes to complete. During FY-25, NCAR PI plans to continue the development of the coupled atmosphere-ocean LES code. This includes running simulations with cold (dense) submesoscale filaments. Also, they plan to simulate boundary-layers typical of the Arabian Sea mini-warm pool focusing on light wind convective periods.

Results Dissemination

The results are disseminated through the journal publication, national and international meetings, conference presentations and invited seminars. A listing of FY24 publications is given below.

Papers Published or in Press: Phadtare, J., Fernando, H.J.S., Krishnamurthy, R., Pe´rez Valent´?n, J.M., McLaughlin, K., Black, G., Dehart, J., Tandon, A., Shroyer, E., Jinadasa, S.U.P., and Bhat, G.S., 2024: Aircraft Observations in a Tropical Supercluster over the Equatorial Indian Ocean during MISO-BOB Field campaign, Scientific Reports, 14, 2182. https://doi.org/10.1038/s41598-024-51527-4. Lozovatsky, I., Escauriaza, C., Suarez, L., Fernando, H.J.S., Coppersmith, R.S., Williams, M., Mayorga, N., 2024: A Snapshot of Marine Turbulence in the Northeastern Strait of Magellan, Ocean Dyn., 74, 459-469. https://doi.org/10.1007/s10236-024-01613-y Lozovatsky, I., Fernando, H.J.S., Jinadasa, S.U.P., and Wijesekera, H., 2023: Eddy diffusivity in stratified ocean: A case study in Bay of Bengal. Environ. Fluid Mech., 23, 1131–1143, https://doi.org/10.1007/s10652-022-09872-3. Luecke, C., Wijesekera,

H.W., Jarosz, E., Wang, D.W., Jensen, T.G., Jinadasa, S.U.P., Fernando, H.J.S., and Teague, W.J., 2023: Characteristics of a Seasonal Front in the Southern Bay of Bengal; Dynamics, Mixing and Water Mass Transport, J. Phys. Ocean., 53(3), 737-761, 2023. DOI 10.1175/JPO-D-22-0070.1. Suarez, L., Guerra, M., Williams, M.E., Escauriaza, C., Lozovatsky, I., Coppersmith, R.S., Fernando, H.J.S., Flow Characterization and Turbulence in the Eastern Section of the Strait of Magellan, Southern Chile, Cont. Shelf Res., In Press. Sullivan, P. P. and McWilliams, J.C., 2023: Oceanic Frontal Turbulence. J. Phys. Ocean., 54, 333-357. Fan, R., Fox-Kemper, B., Suzuki, N., Li, Q., Marchesiello, P., Auclair, F., Sullivan, P.P., and Hall, P., 2024: Comparison of Coastal and Regional Ocean Community Model (CROCO) and NCAR-LES in non-hydrostatic simulations. Geoscien. Model Dev., 17, 4095-4113. Oguejiofor, C. N., Bryan, G.H., Rotunno, R., Sullivan, P.P., and Richter, D.H., 2024: The role of turbulence in an intense tropical cyclone: Momentum Diffusion, Eddy Viscosities, and Mixing Lengths. J. Atmos. Sci., 81,1343-1369. Mazella, E., Hara T., and Sullivan, P.P., 2024: Reduction of Drag Coefficient due to Misaligned Wind-Waves. J. Geophys. Res. (Oceans), 129,1-22. Kimura, Y. and Sullivan, P.P., 2024: 2D and 3D Properties of Stably Stratified Turbulence. Atmosphere, 15,82. Fan, Y., Yu, Z., Sullivan, P.P., and Rydbeck, A., 2024: Dependence of Dense Filament Frontogenesis in a Hydrostatic Model. Ocean Model., 191,102429.

In Revision: Mironov, D.V. and Sullivan, P.P., 2024: Turbulence Structure and Mixing in Strongly Stable Couette flows over Thermally Heterogeneous Surfaces: Effect of Heterogeneity Orientation. Flow Turb. Combus., Revised.

Submitted: Gonzalez, E., Balasubramanian, S., Phadtare, J., and Fernando, H.J.S., Interaction of Atmospheric Cold Pools with Background Flow: A Laboratory Study, submitted to J. App. Meteor. Climatology. Sullivan, P.P., McWilliams, J.C., and Patton, G.E., 2024: An Investigation of Coupled Atmospheric and Oceanic Boundary Layers using Large Eddy Simulation. Submitted to J. Atmos. Sci.. Soni1, A., Soyam, P.S., Bankar, S., Prabhakaran, T., Fernando, H.J.S., Gamage, D., Modjeski, G., Bolella, S., Goes, J., Kovach, C., Bera, S., Arvindhavel, A., Zaffoli, M.L., Tandon, A., Konwar, M., Murugavel, P., Safai, P., Decessari, S., Facchini, M.C., Lee, C.M., and Kalarikkal, N., Regurgitation of Black Carbon Aerosols from the Ocean during a Cyclone" Submitted to Sci. Tot. Environ.

Invited Conference Presentations: Fernando, H.J.S., Sensing Hydrometeorological Processes from Global to Microphysical Scales, Keynote Speaker, 10th International Conference on Environmental Hydraulics, University of Aberdeen, 25-27 June 2024. Sullivan, P.P., Turbulent Marine Boundary Layers: Winds, Waves, and Simulations, ONR MURI, Study on Air-Sea Coupling with Waves, Turbulence and Clouds at High Wind (SASCWATCH), University of Note Dame, South Bend, IN, July 9, 2024 [invited].

Conference Presentations: Wijesekera, H.W., Teague, W., Hallock, Z., Wang, D.W., Luecke, C., Jarosz, E., Jensen, T., Fernando, H.J.S., and Jinadasa, S.U.P., Near-Inertial Waves, Eddies and Mixing in the Thermocline in the Bay of Bengal, Paper # 34C-212, AGU Ocean Sciences Meeting, New Orleans, La., 18-23 February 2024 Gamage, D., Bolella, S., Modjeski, G., Phadtare, J., Thompson, E.J., Tandon, A., Lee . C., and Fernando, H.J.S., Influence of a Dry Air Layer Aloft during the Decay Phase of Arabian Sea Mini Warm Pool, Paper # AI52A-01, AGU Ocean Sciences Meeting, New Orleans, La., 18-23 February 2024 Bollela, S., University of Notre Dame, Notre Dame, IN; and Gamage, D., Modjeski, G., Phadtare, J., Thompson, E.J., Tandon, A., Lee, C.M., and Fernando, H.J.S., Influence of Tropical Cyclone Biparjoy on Arabian Sea Mini Warm Pool: Insights from EKAMSAT Pilot Cruise Paper, S243, 104th AMS Annual Meeting 28 Jan to 1 February, Baltimore, MD, 2024 Sullivan, P.P., Coupled Submesoscale and Ocean Boundary-Layer Turbulence, AGU Ocean Sciences Meeting, New Orleans, La., 18-23 February 2024]

Seminars: Sullivan, P.P., Coupled Submesoscale and Ocean Boundary-Layer Turbulence, Center for

Environmental & Applied Fluid Mechanics, Johns Hopkins University, Baltimore, MD, April 5, 2024 [Invited] Fernando, H.J.S., Sensing Across the Hydrometeorological Spectrum, Mechanical and Aerospace Engineering, University of California, San Diego, 26 February, 2024 [Invited]

Honors and Awards

Peter P. Sullivan was chosen by the American Meteorological Society for the "Award for Outstanding Contributions to Boundary Layer Meteorology." His citation reads: For pioneering work in developing highly reliable large eddy simulations for innovative applications to the atmospheric and oceanic boundary layers and air-sea interactions

PI Fernando shared the 2024 Annual Alan Berman Research Publication Award with a collaborator group at the Naval Research Laboratory, Stennis.

Training Opportunities

Three STEM students from University of Notre Dame (UND) participated in the project: Devmi Gamage (third year PhD student), Selina Bolella (second year PhD student), Owen Diamond (sophomore undergrad from Aerospace Engineering). Post-doctoral fellow Jayesh Phadtare closely engaged in research, investigating the influence of large-scale, sub-seasonal forcing on MWP evolution. Two graduate students (Leg 2) and post-doctoral fellow (Legs 1 and 2) participated in the EKAMSAT-2024 cruise, and were key to data gathering and analysis. As was in the 2023 Pilot cruise, Selina Bolella was the unofficial weather forecaster of the 2024 cruise, and played an important role in leading weather discussions. All UND participants interacted closely with other cruise participants during and after the cruise. Dr. Edgar Gonzales, a Notre-Dame PhD student before the cruise, travelled to Australia to help with the instrument mobilization. Now, he is a National Research Council post-doc at the Naval Research Laboratory NRL (Stennis), and his hire highlights the close collaboration between UND and NRL (Fig. 1). Collaboration with NRL will be further fostered during the 2025 cruise, where coordinated instrument deployments are planned between NRL (Stennis), NRL (Monterey) and UND. Drs. Elisabeth Thompson and Ludovic Bariteau from NOAA Physical Science Laboratory have been generously assisting with the flux-mast development/deployment for all EKAMSAT cruises, a partnership that is invaluable. Undergraduate student Owen Diamond is currently helping with the design and construction of motion-compensating platforms for Lidars and Radar. He is supervised by Research Engineer Scott Coppersmith.

Technology Transfer

The PI is coordinating closely with NRL Stennis (Dr. Hemantha Wijesekera) and NRL Monterey (Drs. Sue Chen and Jerome Schmidt) in deploying instrumentation during the final EKAMSAT cruise in 2025. Their sensor platforms will complement each other and are carefully selected to observe as wide a parameter range as possible. Also, arrangements are being made for instrument inter-comparisons. Grad student Selina Bolella plans to spend a month each at NRL (Monterey) and NRL (Stennis). Both organizations are providing logistical and transportation support for the UND Group at EKAMSAT-2025.

Participants

Name	Role	Person Months
Sullivan, Peter	Co PD/PI	2
Bolella, Selina	Graduate Student (research assistant)	12
Gamage, Devmi	Graduate Student (research assistant)	12
Coppersmith, Ronald	Other Professional	3
Fernando, Harindra	PD/PI	2
Hyde, Jay	Technician	3
Diamond, Owen	Undergraduate Student	1

Upload Document: Figures and Publications

Table 1: Overview of UND instrumentation operated during Legs 1 and 2.

Instrument	Measurement
Inter Met iMet4 Rawinsonde System (403 MHz Sensors). Leg 1 - 00, 06,12, and 18 UTC (every six hours daily), starting from 27 April, 00:00 UTC. Leg 2 -00:00, 04:00, 08:00, 12:00, 16:00 and 20:00 UTC daily (every four hours), starting from18 May 2024, 00:00 UTC	Meteorological Parameters: Environmental temperature, Dew point temperature, Mixing ratio, Relative Humidity, Density, Wind speed, Wind direction, Zonal wind component, Meridional wind component. A total of 60 radiosondes were launched in Leg 1 and 140 in Leg 2.
Optical Disdrometer (Eigenbrodt ODM470)	Particle Size Distribution Precipitation Accumulation
Forward Scatter Sensor (Vaisala FD70)	Present weather sensor for visibility and precipitation.
Vaisala CL 61 Ceilometer	Attenuated Aerosol Backscatter Profiles Cloud Base Heights Linear Depolarization Ratio
NOAA Bow Mast System; Vaisala-HMT337 temperature humidity sensor; Optical Scientific Inc Optical Rain Gauge; Vaisala-PTB220 shielded pressure sensor; Gill Instruments R3 3-axis sonic anemometer; Eppley Precision Spectral Pyranometer PSP Hemisphere GPS VS-1000 system	Pyranometer - Downwelling shortwave radiative flux; Pyrgeometer - Downwelling longwave radiative flux; pressure; GPS handling system; Vaisala WXT520 Weather Transmitter - Temperature, RH, pressure, rain and wind speed/direction (@ 1Hz) at 18m above the surface; LiCOR 7500A - Water vapor (@10Hz) at 18m above the surface; Gill R3A - 3D wind velocity @10Hz;
Micro Rain Radar	Rain rate, drop size distributions, radar reflectivity
Sea Snake (Provided by NOAA PSL)	Approximate Sea Surface Temperature (SST) [-0.05m]
Remote Ocean Surface Radiometer	Skin SST
Vertical Microstructure Profiler VMP250	Ocean Microstructures
Halo Photonics Streamline Scanning Doppler Lidar System + Motion Stabilizing Platform	3-D Wind Velocities and turbulence retrievals

Figure 1: Orson Hyde (UND), Edgar Gonzales (UND) and Ludovic Barriteau (NOAA, PSL) travelled to Freemantle, Australia, during 01-09 April for mobilization of instruments on TGT, in preparation for ASTral-2024. https://psl.noaa.gov/spotlight/2024/astral_install.html The demobilization occurred in Guam.

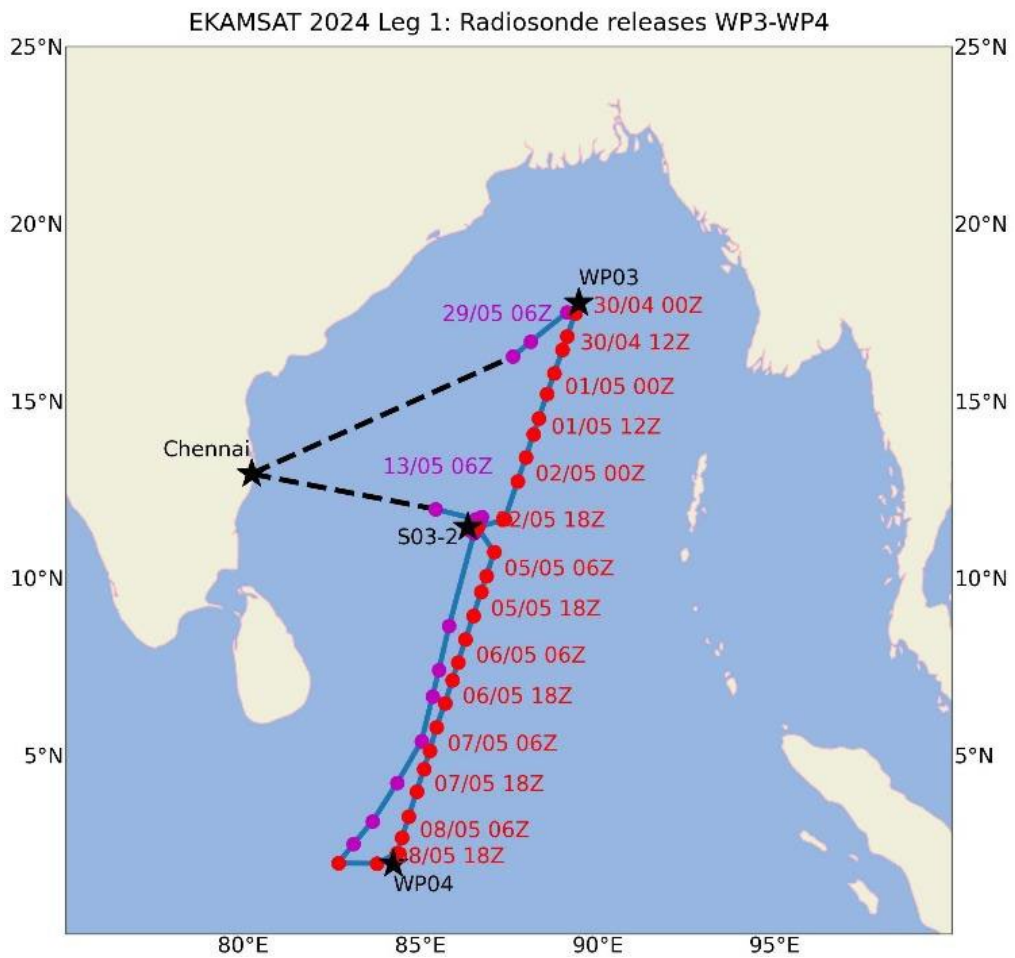

Fig 2a: Leg 1, Ship track (solid) with radiosonde release locations (dots). Red dots - releases for north-south transect of BoB

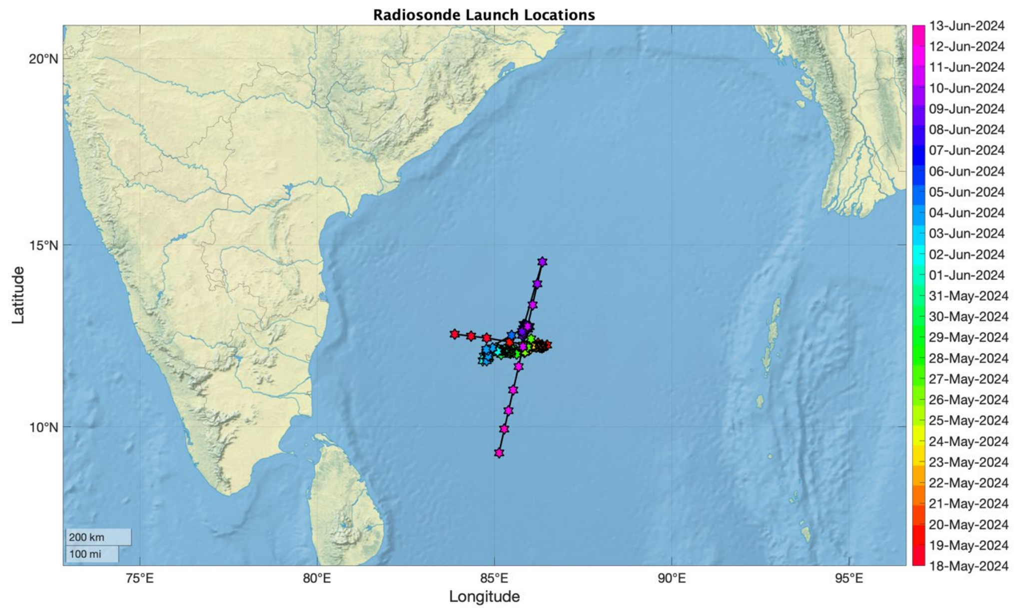

Figure 2b: Leg 2, Ship track, with color-coded stars marking radiosonde launch locations by the date

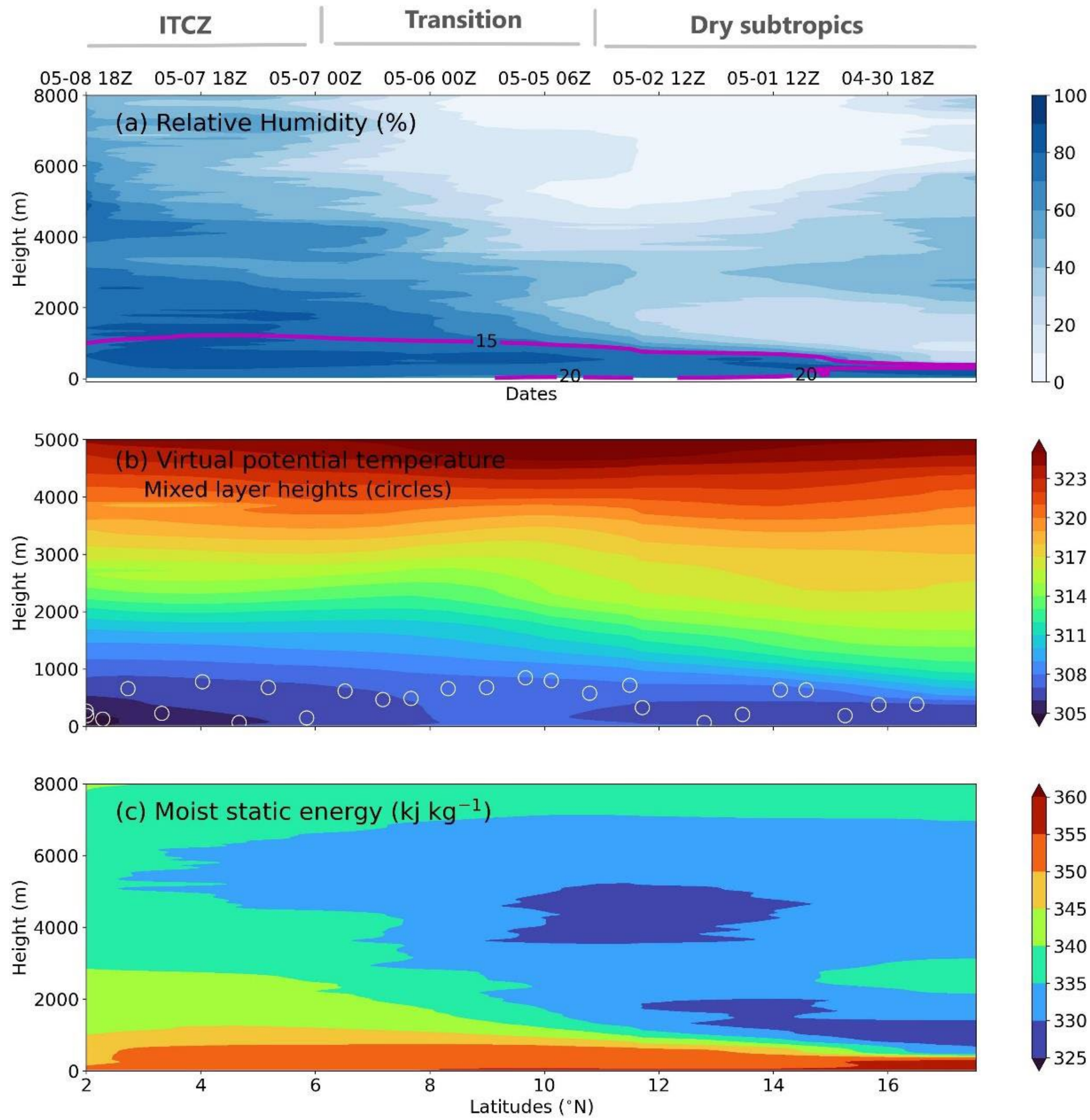

Figure 3: Vertical cross-section of the atmosphere along the north-south TGT track based on the radiosonde observations: (a) Relative humidity (RH), (b) Virtual potential temperature, (c) Moist static energy. The white open circles in (b) show the instances of the radiosonde release (x-axis) and the corresponding mixed layer heights (y-axis).

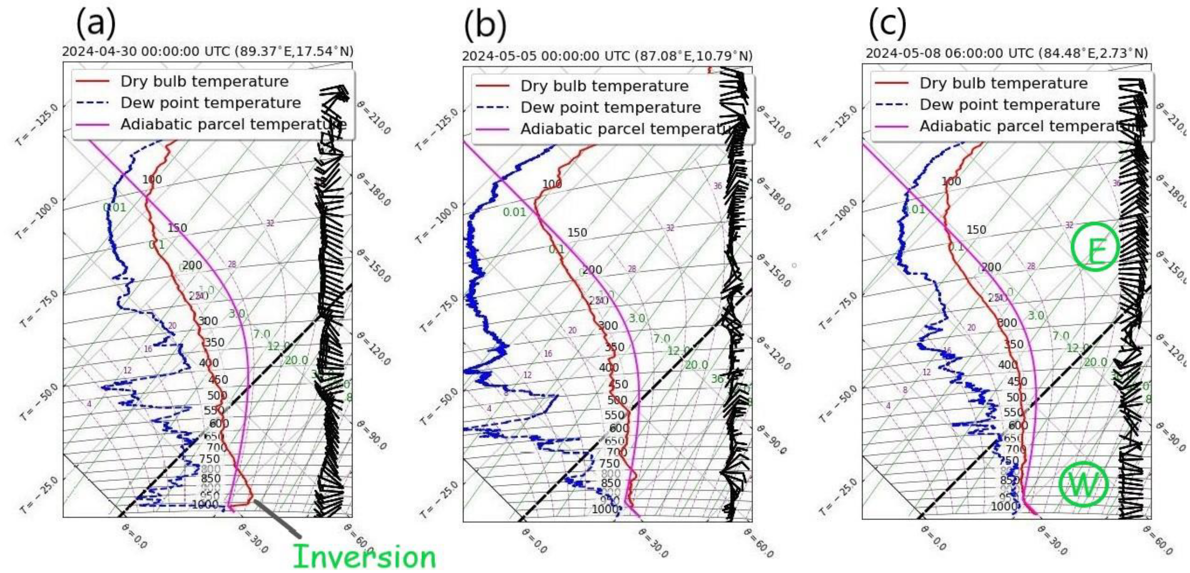

Figure 4**:** Radiosonde soundings tephigrams: (a) 0000 UTC 30 April, (b) 0000 UTC 05 May, (c) 0600 UTC 08 May 2024.

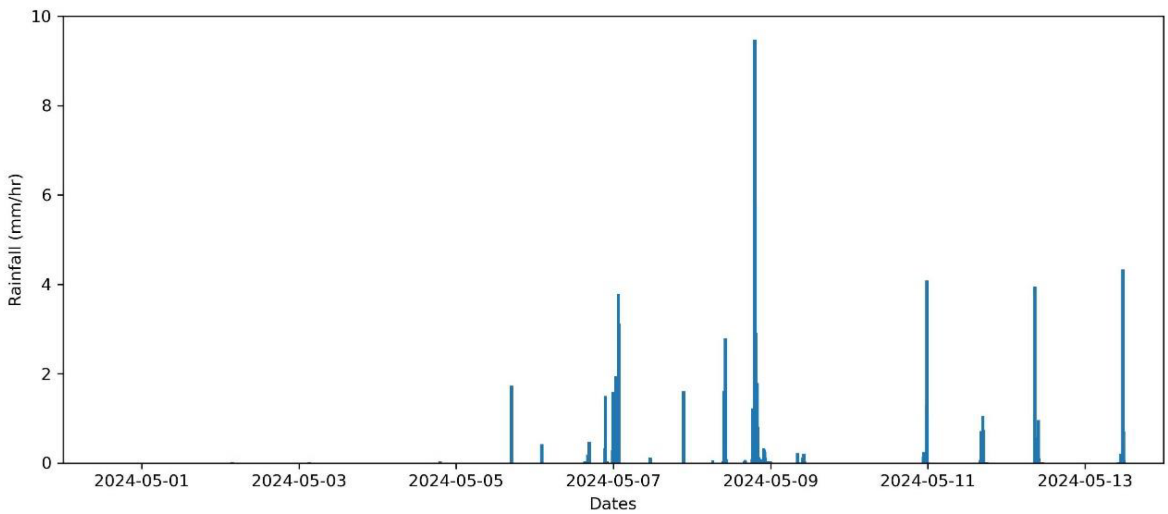

Figure 5: Rainfall intensity from the Present Weather Sensor (FD70)

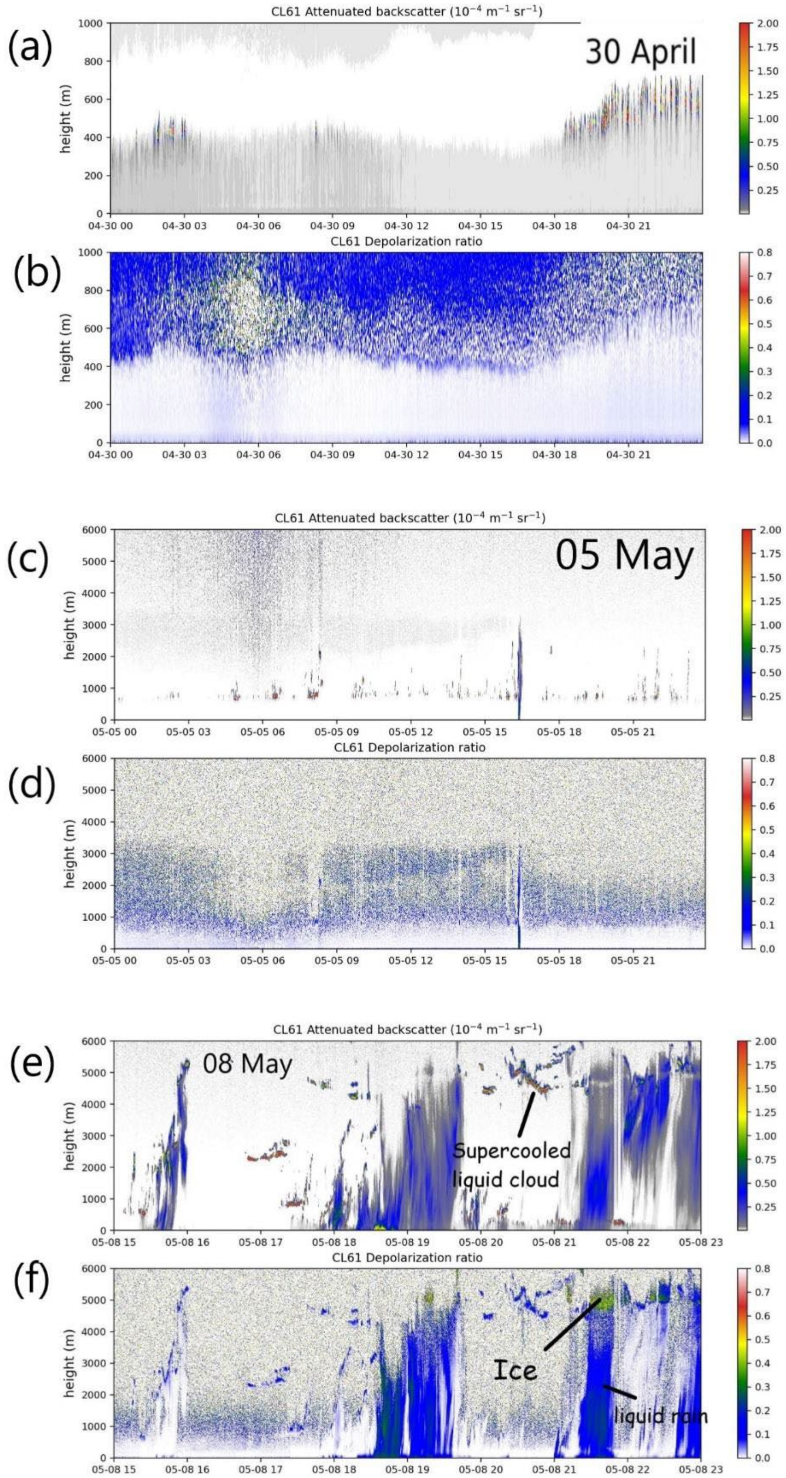

Figure 6: Ceilometer CL61 observations: (a) Backscatter and (b) Depolarization ratio on 30 April; (c)-(d) are the same as (a) -(b) but on 05 May; (e)-(f) Same as (a)-(b) but on 08 May 2024.

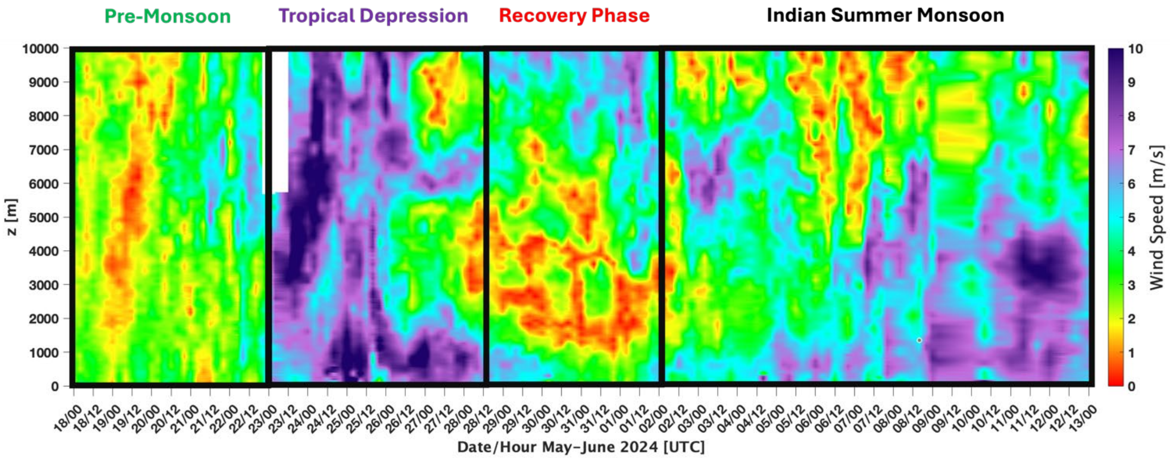

Figure 7: Radiosonde wind speed profile along the ship track from May 18 to June 13, 2024.

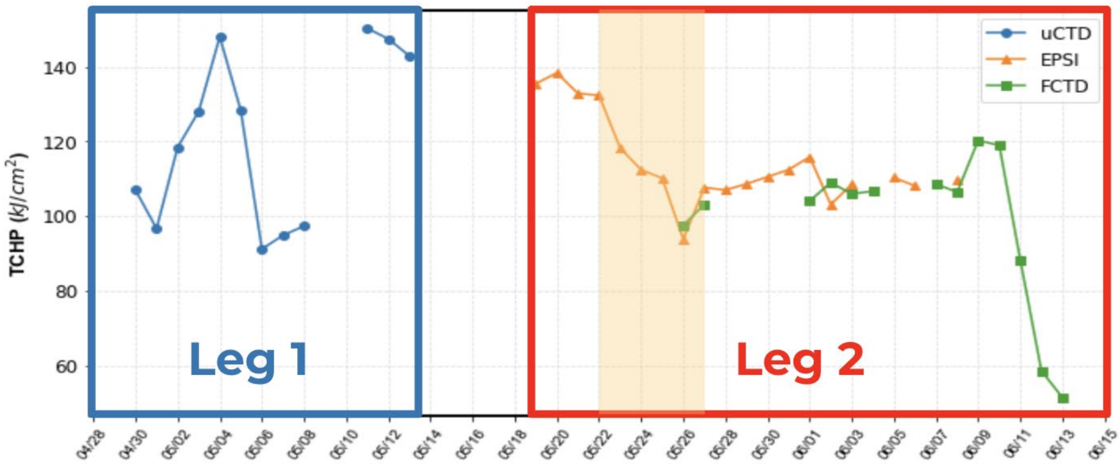

Figure 8: Tropical Cyclone Heat Potential calculation for EKAMSAT-2024 cruise on TGT (April 28 - June 13). Observations are missing for May 10 due to the vessel's speed. In Leg 1 (*blue square*), the uCTD was operated, and the TCHP calculation is shown (*blue line*). In Leg 2 (*red square*), the Epsilometer (*orange line*) and Fast Conductivity Temperature Depth (FCTD) profiler (*green line*) were utilized for calculations. The light orange region highlights the cyclone duration. TCHP is the vertically integrated heat content (based on temperature profile) from the sea surface to the depth of the 26°C isotherm. Both instruments were operated by the Scripps Institution of Oceanography.

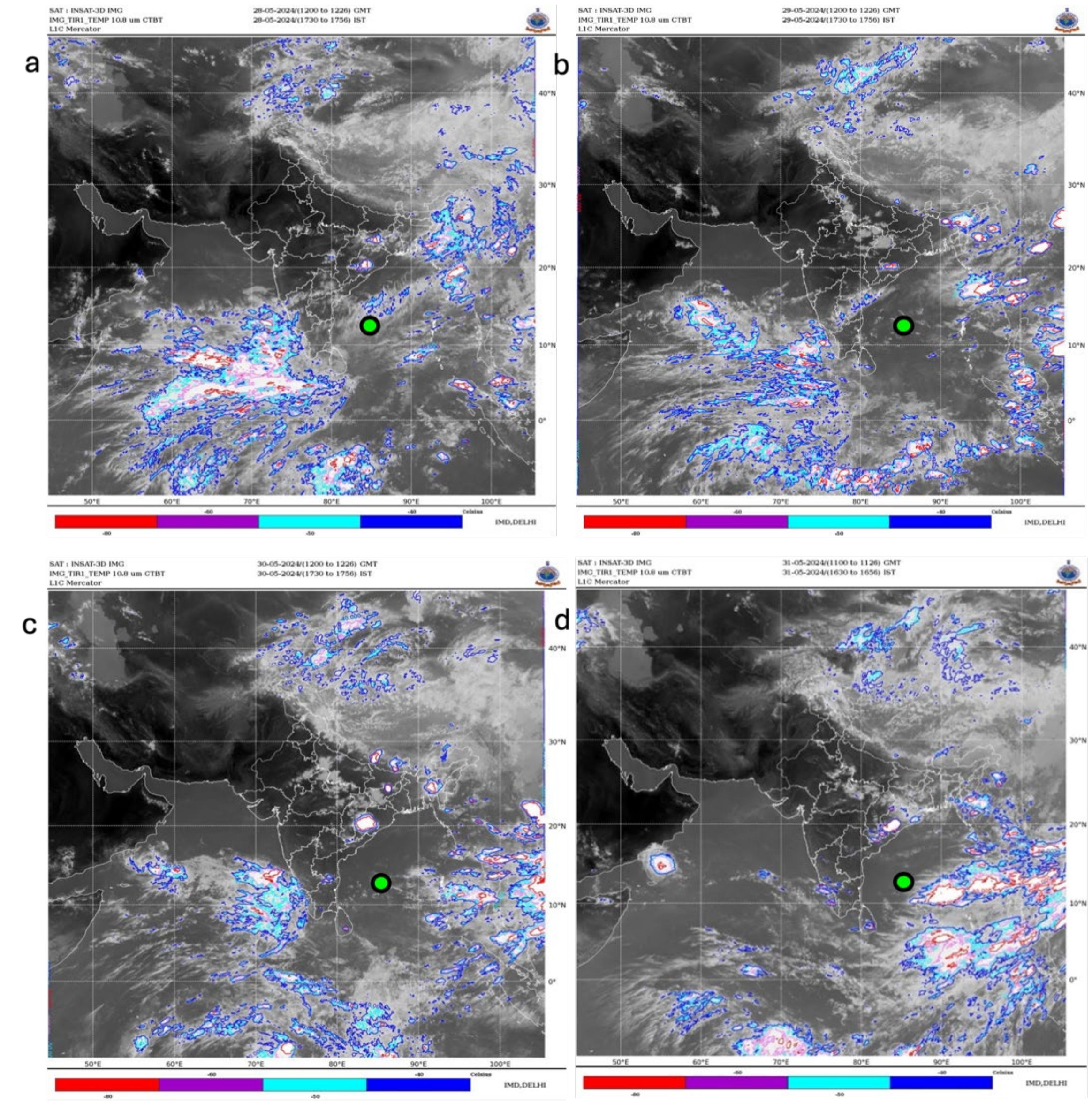

Figure 9: Cloud top brightness temperature (CTBT) during the recovery period as retrieved from INSAT-3D for the following dates and times: a) 28 May 2024, 12:00 UTC; b) 29 May 2024, 12:00 UTC; c) 30 May 2024, 12:00 UTC; d) 31 May 2024, 11:00 UTC.

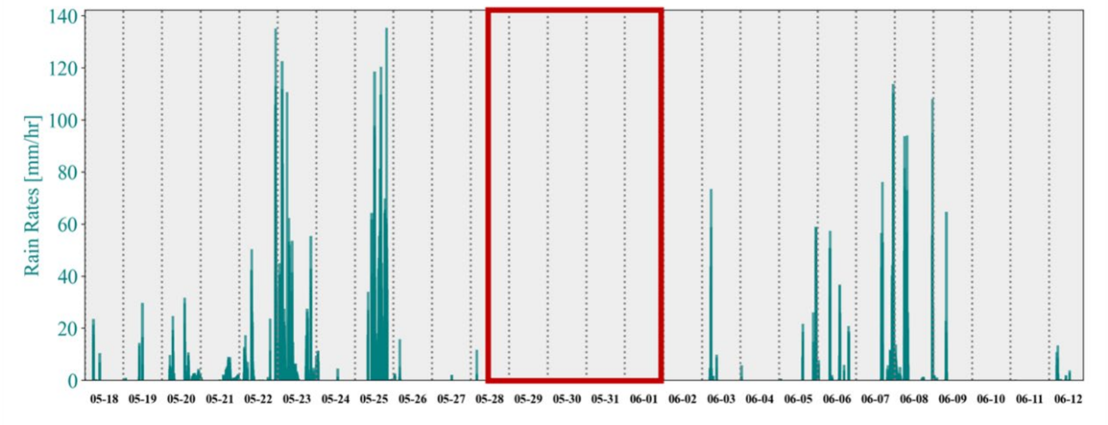

Figure 10: Precipitation rates derived from particle size distribution and terminal velocities obtained from the ODM 470. Red box shows the Recovery period.

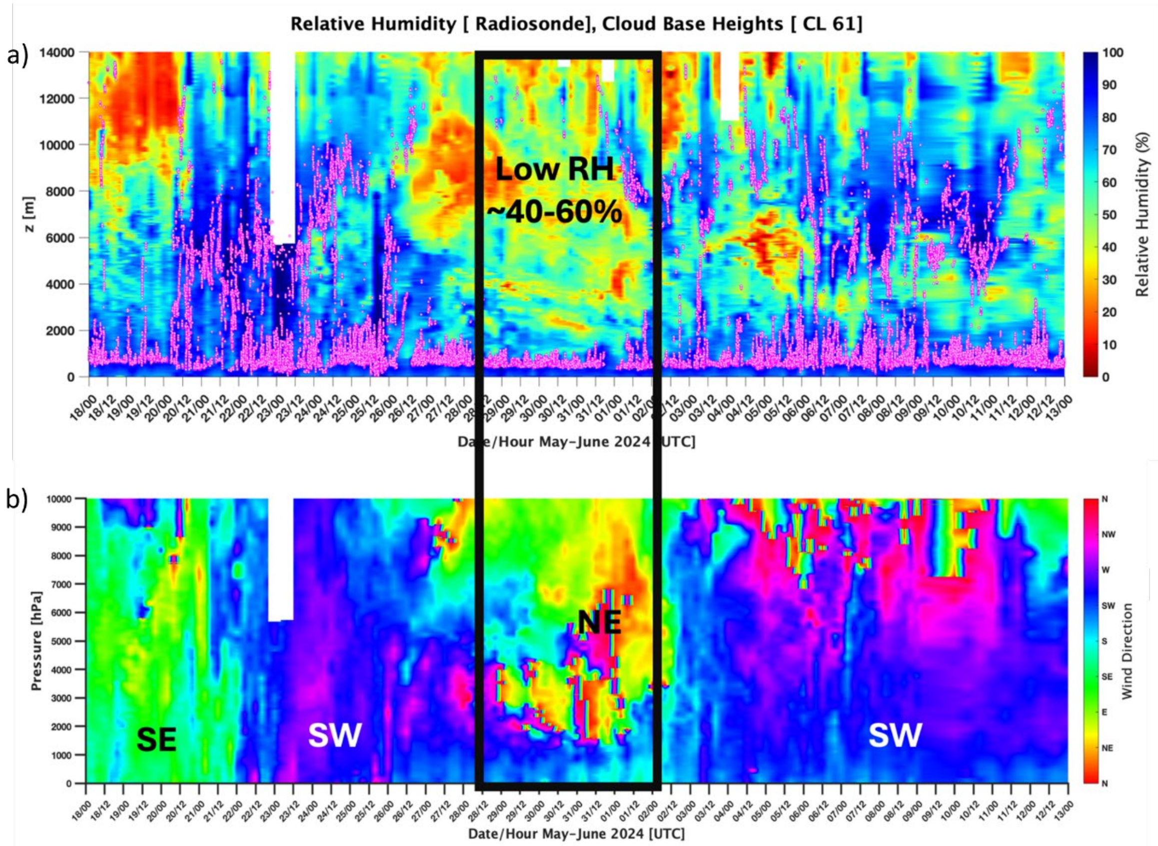

Figure 11: (a) The relative humidity profile derived from rawinsonde measurements, overlaid by CL 61 cloud base heights (b) Wind direction profiles obtained from the radiosonde data.

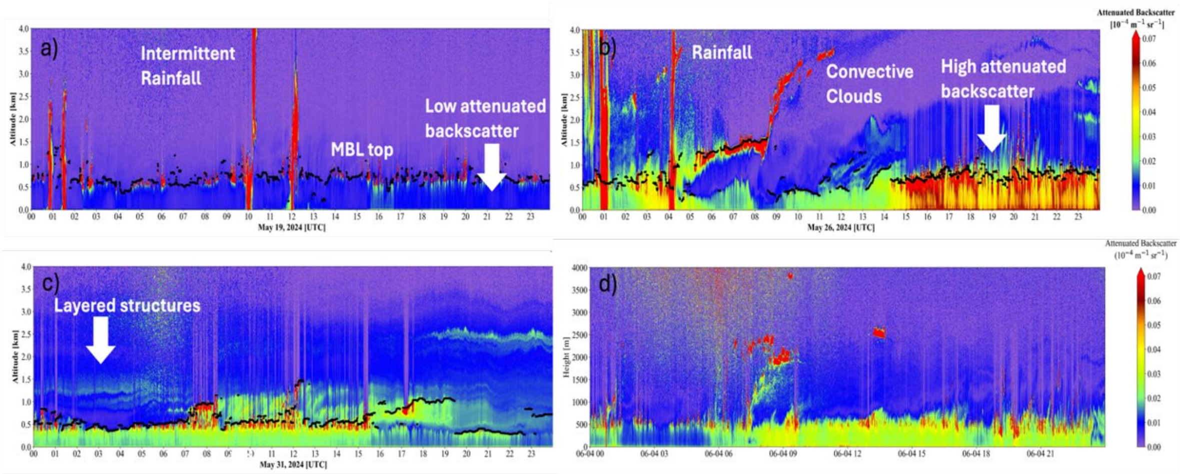

Figure 12: Backscatter attenuation profiles for (a) 19 May 2024, (b) 26 May 2024, (c) 31 May 2024, (d) 04 June 2024. The black markers indicate the marine boundary layer height.

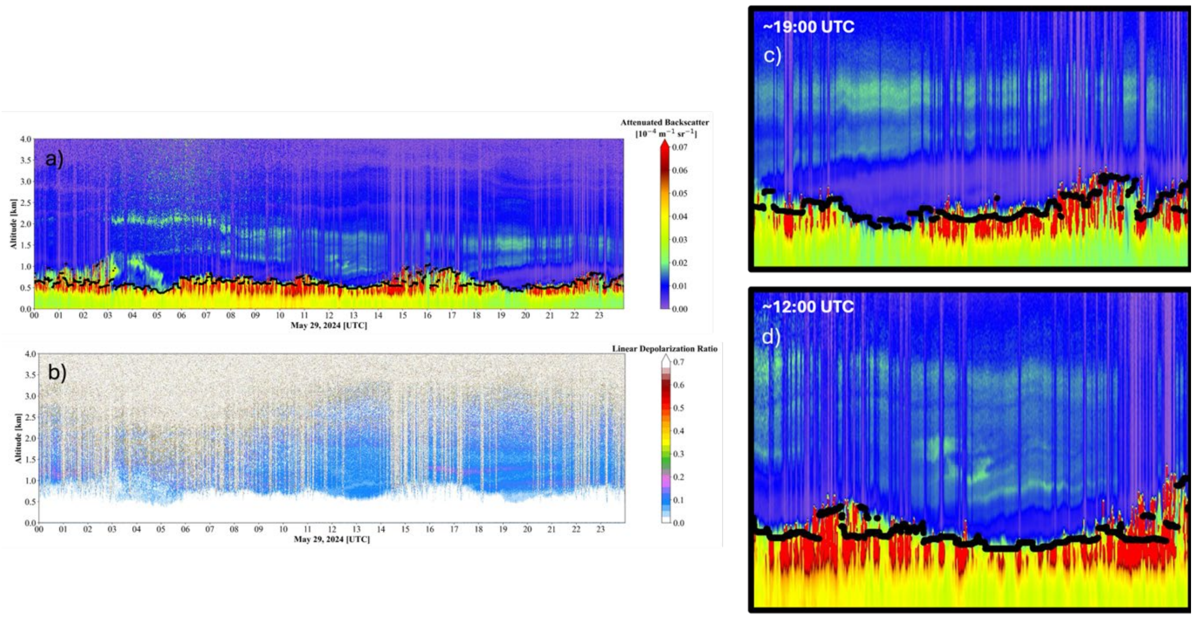

Figure 13: CL-61 atmospheric profiles for 29 May, 2024 (a) Attenuated backscatter profile, (b) Linear depolarization ratio, (c) and (d) zoomed in view of the layered (backscatter) features

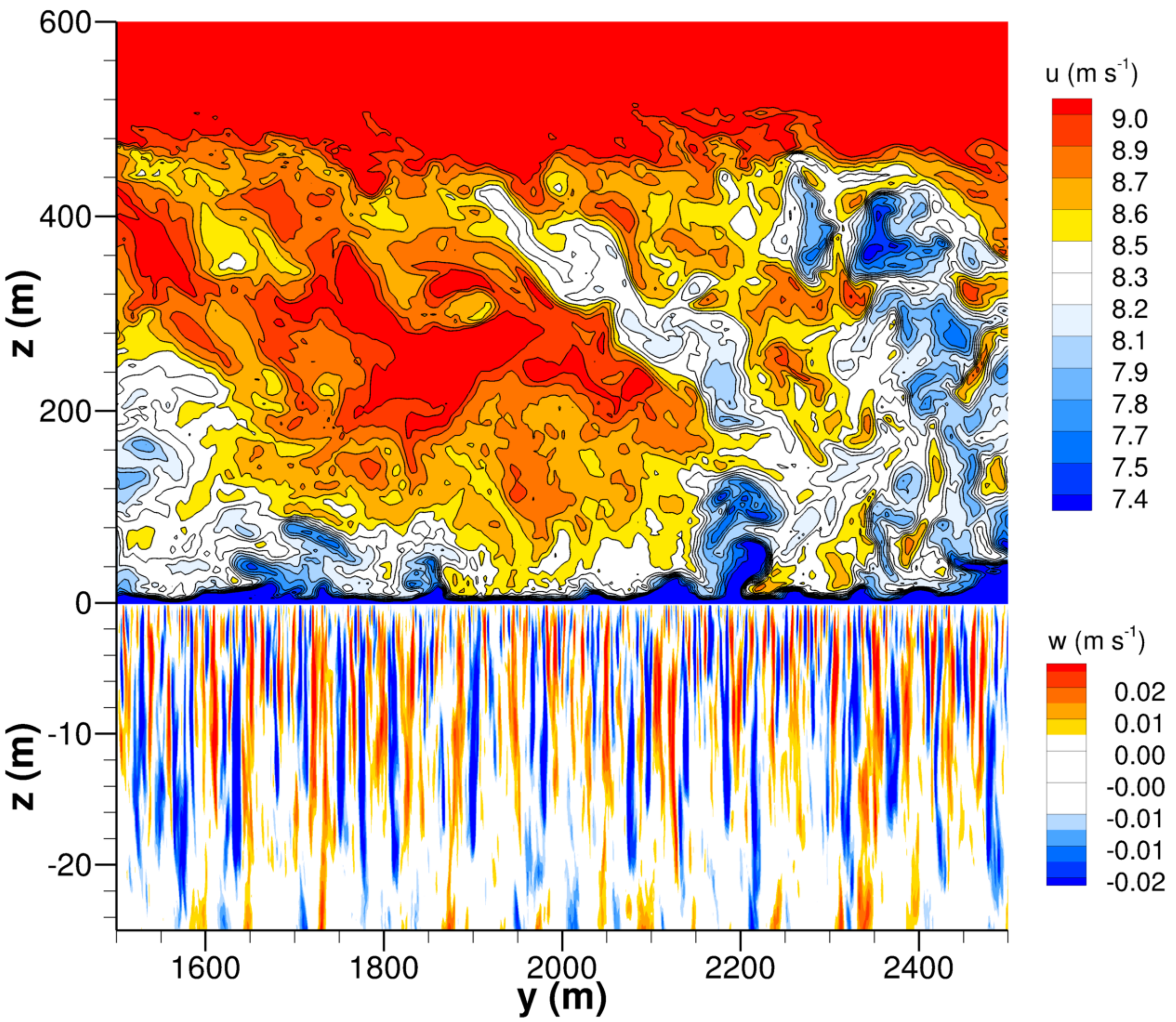

Figure 14: Snapshot of LES results in a (y-z) plane (z = vertically up) from a coupled ABL-OBL simulation driven by geostrophic winds of 10 m s^{-1} and virtual potential surface buoyancy flux of 0.018 K m s^{-1}. Streamwise velocity u in the ABL is shown in the upper panel over z = [0,600] m and, simultaneously, the vertical velocity w in the OBL is shown in the lower panel over z = [-25, 0] m. For clarity, only a fraction of the 5 km y-domain is shown; the z axis in the OBL is expanded compared to the ABL. Notice the coherent structures in the flow. Note a large downdraft in the ABL centered over the region y = [1600 - 2200] m, a signature of ABL shear-convective turbulence, and a small-scale updraft-downdraft pattern characteristic of Langmuir turbulence in the OBL. There is a hint of internal wave generation below the thermocline.

The atmospheric LES uses a mesh of (512, 1024, 256) points and oceanic LES uses (2048, 4096, 128) points. The horizontal dimensions of the LES box, (2.5, 5) km, are discretized with (512, 1024) points in the ABL and (2048, 4096) points in the OBL. The LES vertical dimension is (1200, -60) m in the (ABL, OBL), respectively. The total number of grid points in the LES is 1.21×10^9. The ABL height is ~ 550 m and the depth of the OBL is ~ 20 m.

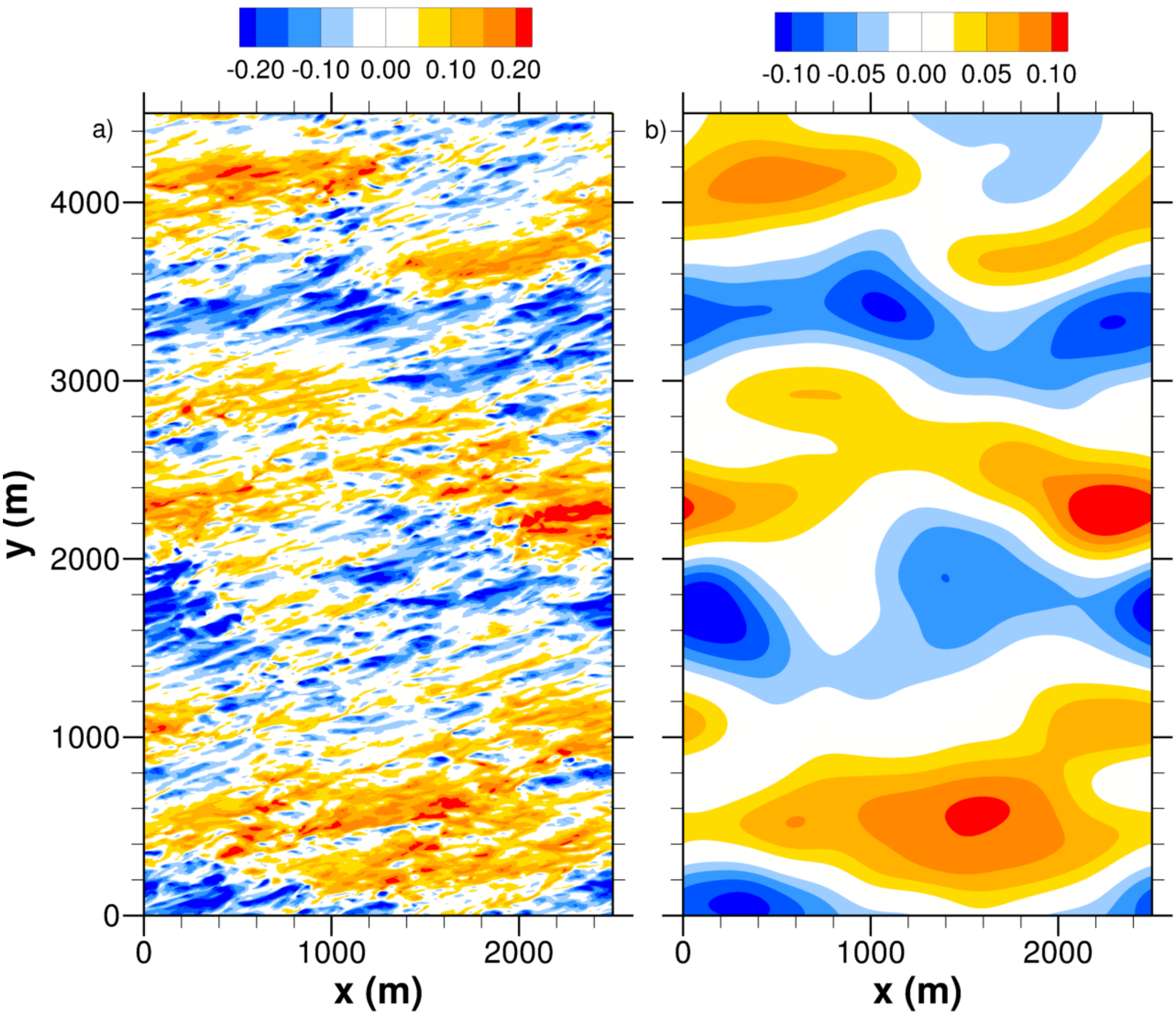

Figure 15: Fluctuating y component of the spanwise momentum stress normalized by the ocean friction velocity squared in the left panel and the filtered normalized fluctuating momentum stress in right panel from a coupled simulation driven by a 10 m s^{-1} geostrophic winds and a surface buoyancy flux 0.035 K m s^{-1}. A two-dimensional Gaussian filter of scale 500 m has been applied to the field in the left panel. Note that the ABL shear-convective rolls leave an imprint on the OBL at large scale.

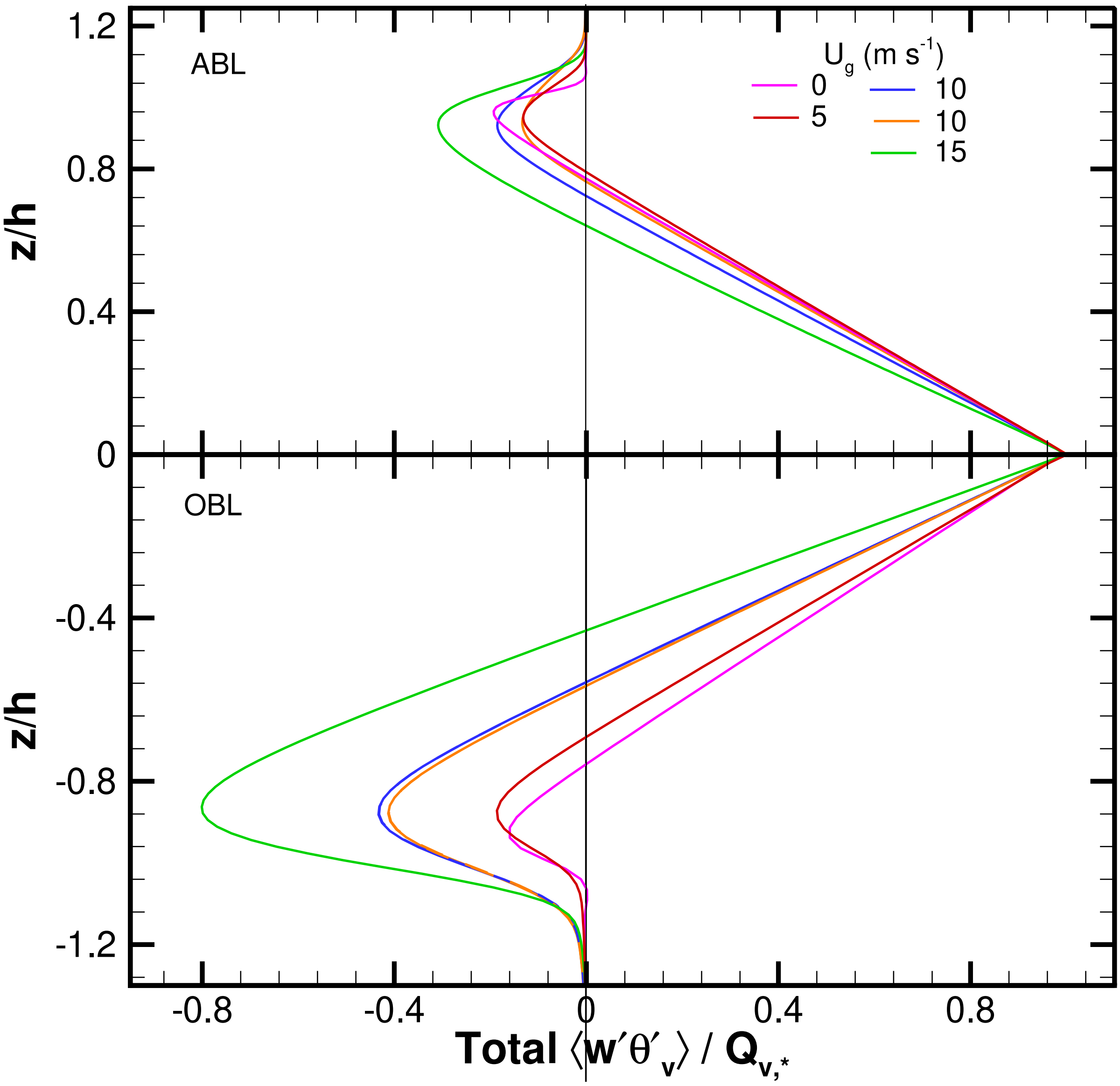

Figure 16: Total (resolved plus SGS) virtual potential temperature flux normalized by surface value in the atmosphere upper panel and in the ocean lower panel. The vertical axis is dimensionless by the ABL or OBL depth. The (solid) colored lines (pink, red, blue, orange, green) correspond to geostrophic winds of (0, 5, 10, 10, 15) m s^{-1} that use point-by-point coupling. The large entrainment flux in the OBL compared to the ABL is a consequence of Langmuir turbulence.